ACS Sustainable Chemistry & Engineering

Research Article

pubs.acs.org/journal/ascecg

Novel Biodegradable Films with Extraordinary Tensile Strength and Flexibility Provided by Nanoparticles

Harpreet Kaur,[§] Tarlok Singh Banipal,[§] Sourbh Thakur,[§] Mandeep Singh Bakshi,*[,†] Gurinder Kaur,[‡] and Narpinder Singh[∥]

[†]Department of Chemistry, Wilfrid Laurier University, Science Building, 75 University Avenue W., Waterloo ON N2L 3C5, Canada

[‡]Nanotechnology Research Laboratory, College of North Atlantic, Labrador City, NL A2 V 2K7 Canada

[§]Department of Chemistry and [∥]Department of Food Science and Technology, Guru Nanak Dev University, Amritsar 143005, Punjab, India

Supporting Information

ABSTRACT: A simple method has been proposed to synthesize environmental friendly biodegradable starch films containing gold (Au) and cadmium sulfide (CdS) nanoparticles (NPs) with significantly improved mechanical properties than pure starch films for various industrial applications. Au NPs were synthesized in vitro by using starch as a weak reducing agent simultaneously for the starch film formation. All reactions were monitored with UV−visible measurements, and it was observed that the growth of Au NPs was proportional to the amount of starch. Due to the inherent surface plasmon resonance (SPR), all Au NP starch films were UV active. Likewise, CdS NPs were synthesized in the glycerol medium and further incorporated in the starch films to make fluorescent active films. X-ray diffraction (XRD), transmission electron microscopy (TEM), atomic force microscopy (AFM), and differential scanning calorimetry (DSC) measurements were used to characterize NPs as well as starch films. A systematic measurement of mechanical properties showed a high degree of tensile strength and flexibility for CdS fluorescent starch films in comparison to Au NP starch films that made the former an ideal candidate for various industrial applications.

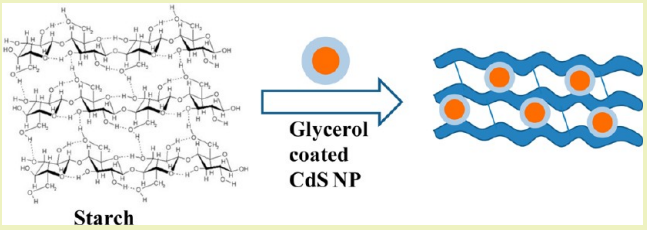

KEYWORDS: *Biodegradable starch films, Nanoparticles, Mechanical properties, Green chemistry*

INTRODUCTION

Uncontrolled use of synthetic polymers (plastics) in different forms has caused great concern about their disposal methods. Economically suited biodegradable materials which can be easily mold into different forms for our day to day life are the best answer to this problem. Such materials can be easily made from starch which is available in large quantities from various plant sources. Starch[1−3] is a polysaccharide primarily made up of amylose and amylopectin with 20−30% and 70−80% respective compositions. Amylose is water insoluble and the main source of our dietary fiber component whereas amylopectin is water-soluble. The presence of amylose makes starch insoluble while amylopectin allows starch to swell in aqueous phase to produce aqueous suspension which can be used to produce biodegradable environmental friendly films with several applications in food and pharmaceutical industries. Several studies[4−12] have been devoted to this aspect and to explore their properties in relation to oxygen barrier, penetration of moisture, tensile strength, and flexibility and have tried to improve them.[13−20] This is all related to the overall molecular arrangement of superhelix amylose and amylopectin and their relative hydration index in relation to retrogradation[21−23] that ultimately determines the film properties. Retrogradation is also known as syneresis where a systematic release of water from a gel state allows linear chains of both amylose and amylopectin to rearrange in a crystalline packing due to hydrogen bonding.

Au nanoparticle (NP) embedded protein films[24−26] show promising mechanical properties when appropriate concentration of NPs is uniformly distributed throughout the protein film in comparison to the film made without them. Likewise, starch complexed NPs[27,28] are expected to influence the retrogradation as well as gelatinization of starch which in turn will dramatically alter the mechanical properties of starch films.[29−32] Starch can easily be procured in comparison to zein protein usually used for making protein films and is better economically suited. We have applied this idea to understand how Au NPs when synthesized in vitro along with starch affect the mechanical properties such as tensile strength and flexibility of starch films and tried to explore their vast applications in food packaging and pharmaceutical industries. For this purpose, we have exploited the weak reducing ability of starch due to its plenty of hydroxyl groups which can reduce Au(III) into Au(0) to generate Au nucleating centers. The NPs thus generated can

Received: July 25, 2012
Revised: November 20, 2012
Published: December 10, 2012

be easily stabilized by starch due to its amphiphilic nature to produce starch conjugated Au NPs in vitro and hence allow homogeneous distribution of NPs throughout the starch gel matrix. A controlled retrogradation entraps NPs in starch gel resulting in the formation of a starch film whose properties depend on the amount, morphology, and size of the NPs. The films thus produced are UV−visible active due to the surface plasmon resonance (SPR)[33,34] of Au NPs. Similarly, fluorescent starch films can also be produced if we use fluorescence active NPs such as CdS. In this case, the synthesis of CdS NPs is not as simple as that of Au NPs, but the overall reaction can be conducted in the presence of glycerol which is used as a plasticizer in the starch film formation. We show here a systematic and comprehensive synthesis of UV−visible and fluorescence active starch films, their characterization, and mechanical properties best suited for their industrial applications.

EXPERIMENTAL SECTION

Starch Isolation. Kidney beans (100 g) were steeped overnight in aqueous toluene solution (2.2 mL/500 mL distilled water) at 40 °C. They were washed, peeled, and ground with distilled water (1:10) to obtain slurry which was passed through a nylon cloth to remove fibers. The residue thus obtained was again ground with distilled water, and the slurry was allowed to stand for 2−3 h. Subsequent washings were given until the supernatant became clear and the starch was procured after drying at 40 °C. Amylose content of the isolated starch was determined by using the method of Williams et al.[35] and found to be 29.5%. It is to be mentioned that even potato starch can also be used instead of kidney bean starch for this study, but it has relatively lower solubility and usually produces less transparent films which may not be suitable for the study of photophysical properties and their subsequent applications as biodegradable fluorescent films.

Synthesis of Starch Conjugated Au NPs. Different amounts of starch (0.5/1/2/5%) were stirred in screw-capped glass bottles at 90 °C for 10 min with constant stirring. The suspension thus obtained in each case was cooled to room temperature and $HAuCl_4$ (0.25/0.5/1.0 mM), from Aldrich, was added. The reaction mixture was kept in a water thermostat bath (Julabo F25) at precisely 70 °C for 6 h under static conditions. The color of the solution changed from colorless to pink−purple after 30 min and remained same thereafter in most of the cases, indicating the formation of Au NPs. The following reaction is considered to take place.

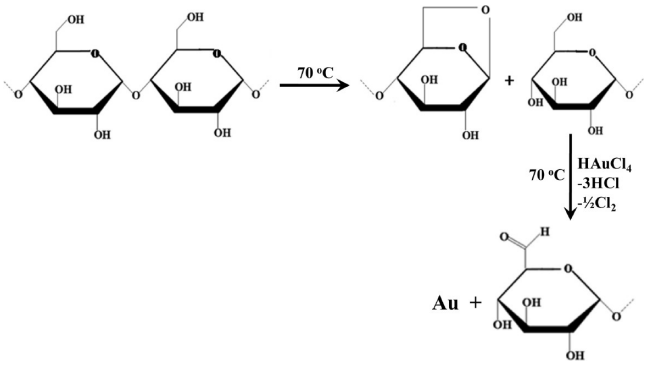

After 6 h, samples were cooled to room temperature and kept overnight. They were purified from pure water at least two times in order to remove unreacted starch. Purification was done by collecting the Au NPs at 10 000 rpm for 5 min after washing each time with distilled water.

Synthesis of Starch Conjugated CdS NPs. CdS nanoparticles were synthesized by taking 10 mL of glycerol in a round-bottom glass flask. Under constant stirring, 1 mL of 0.5 M aqueous acetic acid was added and followed by the addition of 0.5 mL of 0.1 M aqueous cadmium acetate solution. After mixing all the components at room temperature, the reaction mixture was kept in an oil bath under precise temperature control of 150 °C at constant stirring. Then, 0.5 mL of aqueous 0.1 M thioacetamide was added and the reaction was carried out for 48 h. The following reaction was considered to take place, and the CdS NPs thus produced were purified as mentioned above in the case of Au NPs.

$$Cd(OOCCH_3)_2 + H_2O \rightarrow CdO + 2CH_3COOH$$

$$CH_3CSNH_2 + H_2O \rightarrow CH_3COONH_4 + H_2S$$

$$CdO + H_2S \rightarrow CdS + H_2O$$

UV−visible and Fluorescence Studies. UV−visible spectra of as prepared colloidal suspensions were recorded by Shimadzu Model No. 2450 (double beam) in the wavelength range of 200−900 nm to determine the absorbance. Steady state and time-resolved fluorescence spectroscopy of especially CdS NP suspensions were carried out by using the PTI QuantaMaster and PicoMaster 2 TCSPC Lifetime Fluorometer, respectively. Both instruments are equipped with a thermoelectrically temperature controlled cell holder that allows the measurement of the spectrum at a constant temperature within ±1 °C.

Film Casting. Starch films embedded with Au or CdS NPs were made directly from the as prepared samples. A 10 g portion of the respective colloidal NP suspension was weighted in a 9 cm diameter plastic Petri dish along with 30% glycerol (starch weight basis) as a plasticizer. For the CdS NP sample, 30% glycerol was accounted for along with the as prepared colloidal NPs suspension. The suspension was then gently swirled to coat the bottom of the dish and was placed on a level surface in an oven at 40 °C for 24 h. Three replicate films were cast for each sample. Dehydration of this filmogenic solution led to a film formation which was easily peeled off. All films were stored in a desiccator over P_2O_5 for at least two weeks to obtain constant weight. Larger films for more practical purposes such as wrapping sheets or bags can also be prepared in a similar fashion as long as the above method is adopted.

Color Coordinates. Color coordinate data of the films were determined using a Hunter colorimeter Model D 25 optical sensor (Hunter Associates). The Hunter *L*, *a*, and *b* color space is a three-dimensional rectangular space based on the opponent color-theory. *L** is a measure of "brightness", while *a** and *b** are the color coordinates that range from −90 to +90 in the color space "circle". For a*, −90 = green and +90 = red, and for *b**, −90 = blue and +90 = yellow. To perform the color tolerance, a standard sample was measured and saved for subsequent comparisons.

Microscopic and X-ray Diffraction Studies. Transmission electron microscopy (TEM) measurements were carried out by mounting a drop of a purified NP suspension on a carbon coated Cu grid and allowed to dry in air. It was observed with the help of a Philips CM10 Transmission Electron Microscope operating at 100 kV. Atomic force microscopic (AFM) measurements of starch films were carried out by model Veeco diCaliber at room temperature. A 5 cm^2 piece of a starch film was placed on an ultra cleaned glass coverslip. It was then scanned with silicon nitride tip in contact mode to get amplitude and height images. Survey scanned images were processed and analyzed by using SPM graphic software to obtain the three-dimensional topography of a starch film. X-ray diffraction (XRD) patterns were recorded by using Bruker-AXS D8-GADDS with T_{sec} = 480. Samples were prepared on glass slides by placing a concentrated drop of purified NP suspension and then dried in a vacuum desiccator. Likewise, XRD patterns of starch films were determined by using separate attachment to hold the film.

Differential Scanning Calorimetry Studies. Thermogravimetric analysis/differential scanning calorimetry (TGA/DSC) of the starch films was carried out on a TA Instruments SDT Q600 using approximately 10 mg sample accurately weighed into an aluminum sample pan. An empty aluminum pan was used as reference. The sample was heated at 5 °C/min heating rate in the temperature range from 20 to 500 °C under air flow (100 mL/min).

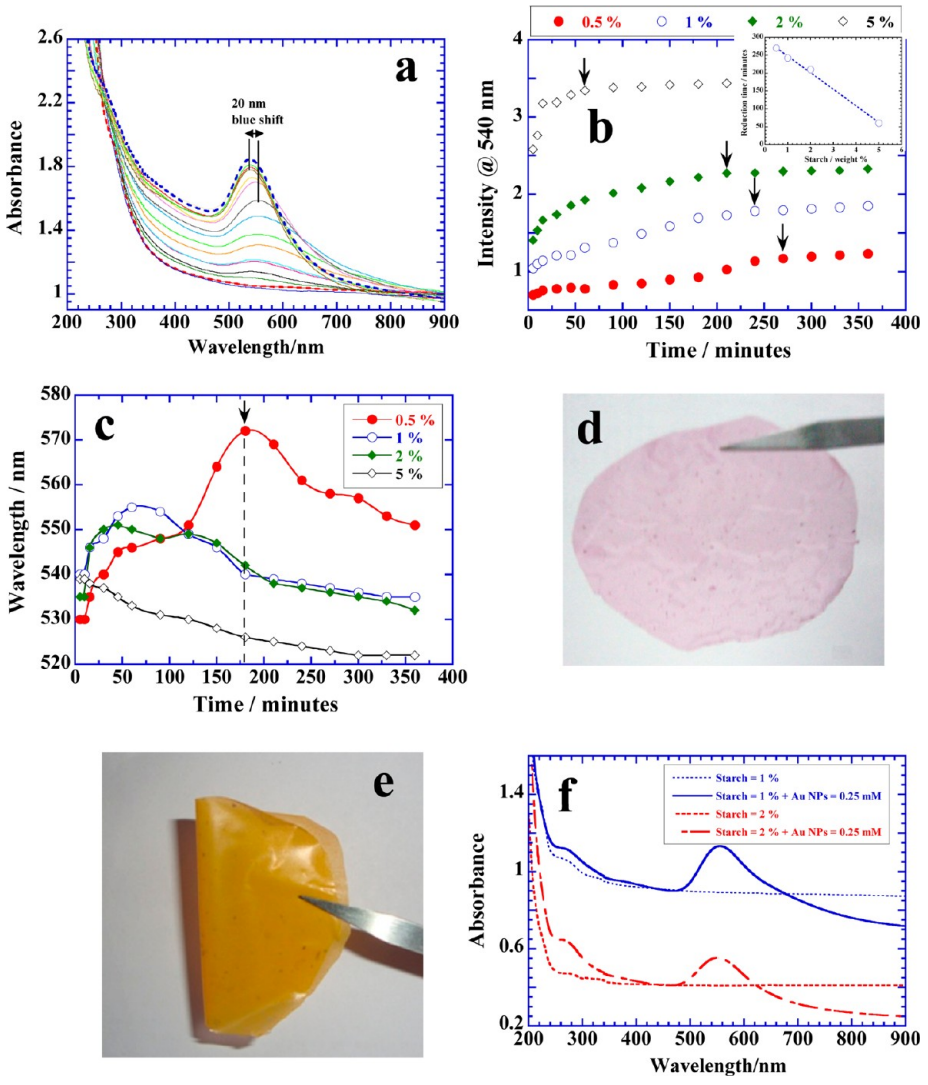

Figure 1. (a) UV−visible scans of aqueous 1% starch and 0.25 mM $HAuCl_4$ at 70 °C with time from 5 min (lowest scan) to 6 h (upper most with dotted line). (b) Intensity at 540 nm of Au NPs versus time plots of reactions with 0.5, 1, 2, and 5% starch and 0.25 mM $HAuCl_4$ at 70 °C. (inset) Linear dependence of reduction time on the amount of starch. (c) Wavelength maximum of the absorbance of Au NPs versus time plots of reactions with 0.5, 1, 2, and 5% starch and 0.25 mM $HAuCl_4$ at 70 °C. (d) Photograph of Au NPs embedded starch film. (e) Photograph of CdS NPs embedded starch film. (f) Absorbance versus wavelength scans of starch films made with and without Au NPs. Note the absorbance around 540 nm due to the presence of Au NPs in the starch films. See details in the text.

Mechanical Properties. The mechanical properties of the films were measured using a Texture Analyzer (TAXT2, Stable Micro-systems, Godalming, U.K.) with a 5 kg load cell. The speed was kept constant at 1 mm/min. A well-defined geometry of each film (with average thickness, width, and length of 0.05, 5, and 50 mm, respectively) was used to measure the tensile properties of each film. The measurements were carried out by fixing the ends of a film to two metal plates by using cyanoacrylate glue. It was then single-edge notched to a depth of 2.5 mm midway along the length. The mechanical tests were performed to obtain force/displacement data, tensile strength (MPa), and strain at failure. Tensile strength was measured using $\sigma = F_{max}/(w - a)t$, where F_{max} is the maximum force associated with failure, w is the width of the strip, a is the notch length, and t is the thickness of the strip. Strain at failure was calculated as $\varepsilon_{fail} = \Delta l_{max}/l$, where Δl_{max} is the change in length at F_{max} and l is the initial length.

RESULTS

UV−visible and Fluorescence Studies. Synthesis of Au NPs was carried out by reducing Au(III) into Au(0) using starch as a reducing agent and monitored simultaneously by the UV−visible measurements. Figure 1a depicts a typical plot where no absorption of aqueous starch is observed in the visible region but, as soon as Au nucleating centers are formed, a peak appears around 540 nm due to the SPR of Au NPs.[8] It becomes more significant with the passage of time. The plot of intensity at 540 nm versus time (Figure 1b) shows an increase in the intensity with time as NPs grow in size before tending to a constant value (indicated by an arrow). This value decreases as the amount of starch increases from 0.5 to 5% in a linear fashion (Figure 1b, inset) which means that the reduction is proportional to the amount of the reducing agent.[36,37] Another important feature of Figure 1a is the overall blue shift of about 20 nm in the absorbance of Au NPs, and its variation with time is depicted in Figure 1c. For a reaction of 0.5% starch, at first it goes through a red shift of about 40 nm which after attaining a maximum value (indicated by an arrow) reverts to a blue shift of 20 nm before tending to a constant value. This variation, though quite clear in the presence of 0.5% starch, diminishes at

dx.doi.org/10.1021/sc3000652 | ACS Sustainable Chem. Eng. 2013, 1, 127−136

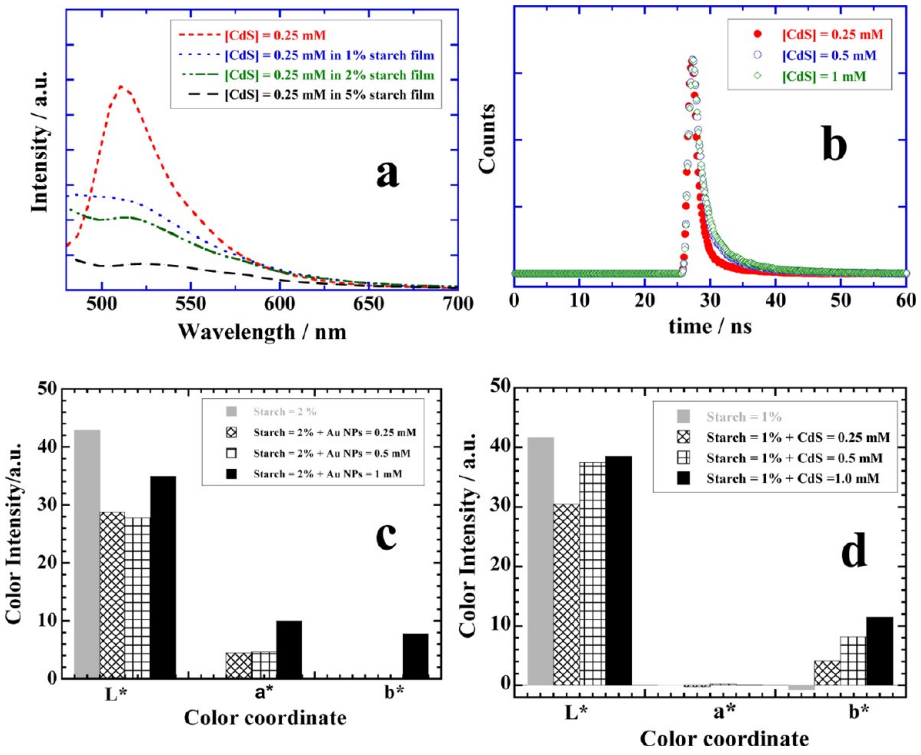

Figure 2. (a) Steady state fluorescence of CdS NPs in suspension and embedded in starch films. Note a relatively weak emission of CdS NPs present in the starch films. (b) Fluorescence lifetime decay of CdS NPs in starch films. (c and d) Color coordinates of 1% starch films made without and with different concentrations of Au and CdS NPs, respectively. See details in the text.

higher amounts, while 5% starch shows no red shift at all. In order to understand this behavior further, we have divided the 0.5% starch curve into two parts: the first part with red shift is related to the nucleation while the second part with blue shift can be related to the association of starch with NPs. The lowest amount of starch (i.e., 0.5%) is expected to generate few nucleating centers which slowly grow under the autocatalytic effect to accommodate unreduced gold ions. This slow growth process is usually accompanied with a red shift because it leads to larger morphologies. In contrast, a greater amount of starch (i.e., 5%) converts the maximum amount of gold ions into nucleating centers with relatively less possibility of further growth; hence, no red shift is observed. The blue shift on the other hand is related to the screening of the SPR of Au NPs upon complexation with starch macromolecules; hence, it happens in all cases with maximum effect for 5% starch because, as soon as the Au nucleating centers are created, they are complexed with the much greater amount of starch (Figure 1c).

For CdS NPs, a simultaneous measurement of UV−visible spectrum at 150 °C was not possible, therefore the absorption of as prepared samples was carried out at room temperature and depicted in the Supporting Information, Figure S1a. A weak band close to 500 nm in observed in all cases due to the yellow color of the CdS NPs.[38] Starch conjugated NP suspensions from both reactions are directly converted into starch films (see the Experimental Section for details) which is usually pink or purple in color in the case of Au NPs (Figure 1d) while it is bright yellow for CdS NPs (Figure 1e). A uniform color of both films indicates that the NPs are evenly distributed throughout the starch film as they were in the colloidal suspensions. The absorbance spectra of starch films with and without Au NPs are depicted in Figure 1f. Clear peaks due to SPR around 550 nm are due to the presence of embedded NPs which are absent in the respective control experiments. Likewise, CdS NPs also show similar absorption bands around 500 nm in their films (Supporting Information Figure S1b) which were previously demonstrated by their suspensions (Figure S1a).

Fluorescence spectra of the CdS NP suspension along with that of the films at an excitation wavelength of 450 nm are shown in Figure 2a. The NP suspension gives a clear emission around 510 nm[39] which increases with the increase in the amount of NPs (Supporting Information Figure S2). Fluorescence emission of CdS NPs in films is suppressed and about 10 nm red shifted (Figure 2a). In addition, a greater amount of starch shows a greater suppression in the emission intensity. Lifetime measurements profiles are depicted in Figure 2b for CdS NP films made with 1% starch. The lifetime decay of CdS NPs in films is fit to multiexponential function with average lifetime between 1 and 3 ns.

Color Coordinates. Color coordinates (Figure 2c) further help us to characterize the color properties on the basis of the isotropic nature of the films.[5] A low value of L^* in the presence of Au NPs of different concentrations can be attributed to the less bright or less transparent starch film in comparison to their absence and is obviously understood from the pink−purple color of the NPs incorporated in films. The a^* value indicates the presence of red color which is provided by the small NPs due to the SPR with absorbance around 540 nm in comparison to the purple color of larger NPs with red shifted absorbance. a^* is maximum for a greater amount of Au NPs (i.e., 1 mM) which is obviously expected due to the presence of a greater number of NPs. The b^* value for this film indicates the presence of weak yellow color which might arise from the semicrystalline nature of starch or to some extent due to unreacted Au(III). It is absent in films with 0.25 and 0.5 mM of

dx.doi.org/10.1021/sc3000652 | ACS Sustainable Chem. Eng. 2013, 1, 127−136

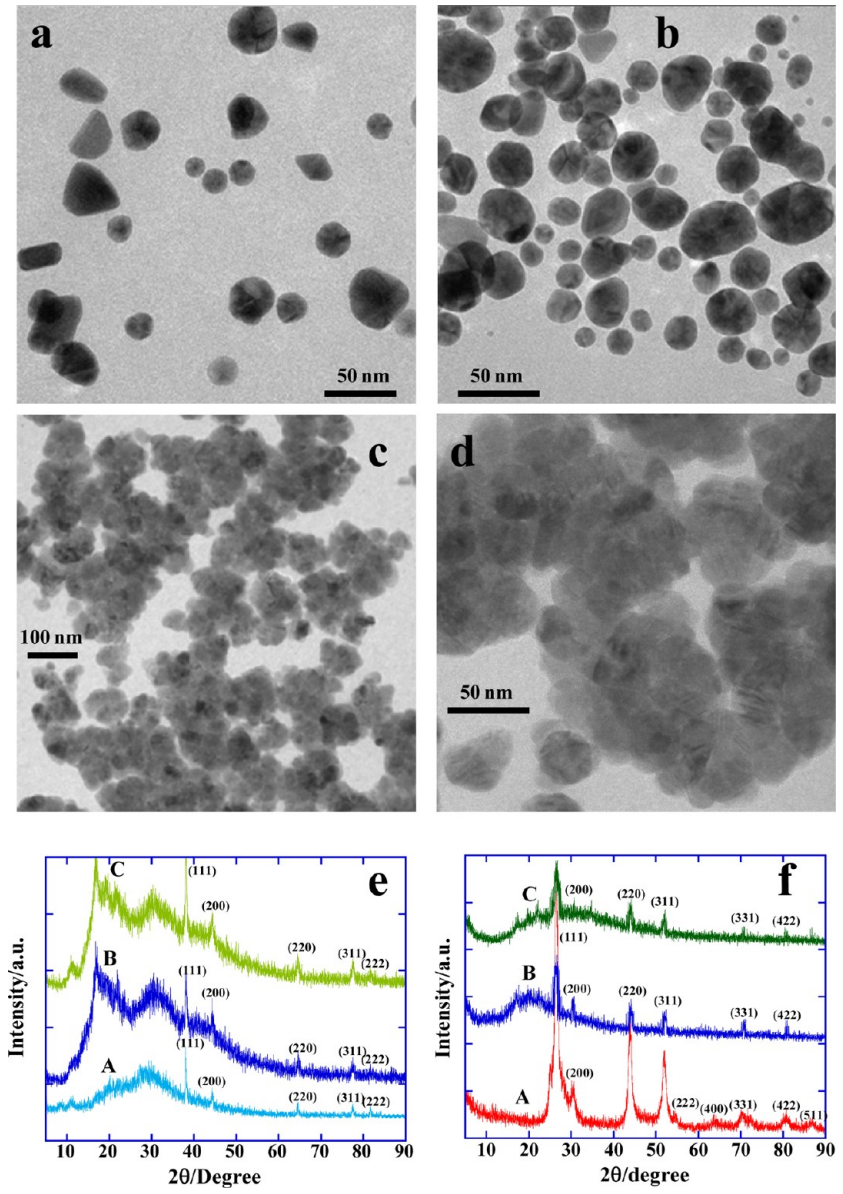

Figure 3. (a and b) TEM micrographs of Au NPs synthesized at 70 °C in the presence of 1% and 2% starch, respectively, along with $HAuCl_4$ = 0.25 mM. (c and d) TEM micrographs of CdS NPs synthesized at 150 °C in glycerol medium. (e) XRD patterns of Au NPs in suspension (A) and in 1% (B) and 2% (C) starch films. (f) XRD patterns of CdS NPs in suspension (A) and in 1% (B) and 2% (C) starch films. See details in the text.

Au NPs which means that almost all gold ions are converted into nucleating centers in these films. Similar behavior is observed for 1% starch films in the absence and presence of Au NPs (Supporting Information Figure S3). In the case of CdS NP starch films, the large b^* values of color coordinates (Figure 2d) demonstrates the presence of strong yellow color due to the presence of fluorescent CdS NPs while insignificant values of a^* can be attributed to the absence of red color contrary to the Au NP films.

Microscopic and XRD Studies. TEM studies help us to understand the morphology of the Au and CdS NPs. Figure 3a and b shows the TEM images of purified Au NPs (see the Experimental Section) synthesized with 1 and 2% starch, respectively, with corresponding EDS spectra indicating the emission due to Au (Supporting Information Figure S4). NPs of polyhedral shapes with comparable sizes of 22 ± 9 and 25 ± 12 nm, respectively, are evident. Polyhedral shapes suggest that starch is a good stabilizing agent but is not a good shape directing agent.[40−42] The latter property stems from an effective liquid−solid interfacial adsorption of a stabilizing agent, and that is not expected for starch due to its weak amphiphilic behavior. However, starch forms a good amorphous film with entrapped NPs in a relatively less purified sample (Supporting Information Figure S5). On the other hand, CdS NPs of about 20 nm exist in the form of small interconnected clusters of about 100 nm (Figure 3c). Close inspection (Figure 3d) suggests that each cluster is made up of 6−10 NPs. XRD patterns of Au NPs (Figure 3e) with and without films are sharp and hence indicate the crystalline nature of NPs with predominant growth at {111} crystal planes of fcc geometry of Au. Likewise, XRD patterns of CdS NPs (Figure 3f) represent crystalline cubic structure with more prominent peaks for NPs in purified suspension rather than in films. Peaks arising at 17° and 22° scattering angles (Figure 3c) belong to conjugated amorphous starch[43−45] and are more prominent for Au NPs films rather than CdS NPs films because Au NPs are

dx.doi.org/10.1021/sc3000652 | ACS Sustainable Chem. Eng. 2013, 1, 127−136

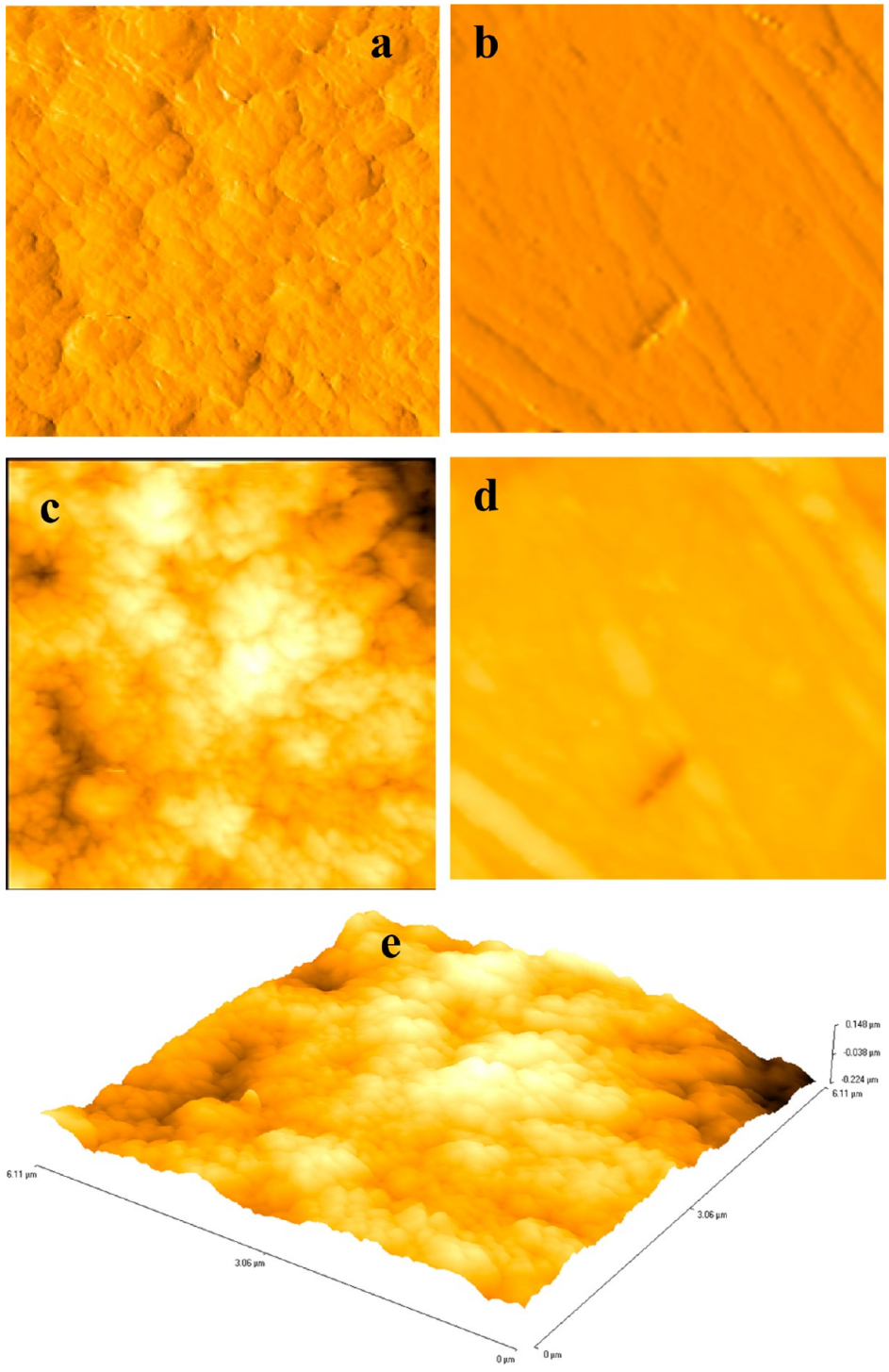

Figure 4. (a and b) AFM images of 1% starch film with and without Au NPs, respectively, showing the surface topography. (c and d) Respective height images along with a surface plot (e). See details in the text.

synthesized in the presence of starch as a weak reducing agent whereas Cd NPs are prepared in the glycerol medium (see Experimental Section). Due to the predominantly amorphous nature of starch films, it is difficult to quantify the effect of NPs on the crystalline arrangement of amylose during the film formation which usually exists in B-type polymorph.[46] The presence of NPs (of ∼12−24 nm) is expected to affect the overall dense double helical arrangement of starch made up of thin lamellar domains of about 4.5 nm thick by intercalating themselves. This effect is expected to be more prominent for Au rather than CdS NPs because Au NPs have been synthesized in vitro. We will correlate this aspect with mechanical properties later in the Discussion section.

AFM studies further help us to understand the surface roughness of the starch films. Figure 4a shows the topography of NPs embedded starch film made with 1% starch. Panel b compares its control, i.e. without NPs. A marked difference can be observed between the topography of two films. The topography of the film incorporating NPs (panel a) clearly shows the presence of peaks and valleys[25] due to embedded

dx.doi.org/10.1021/sc3000652 | ACS Sustainable Chem. Eng. 2013, 1, 127−136

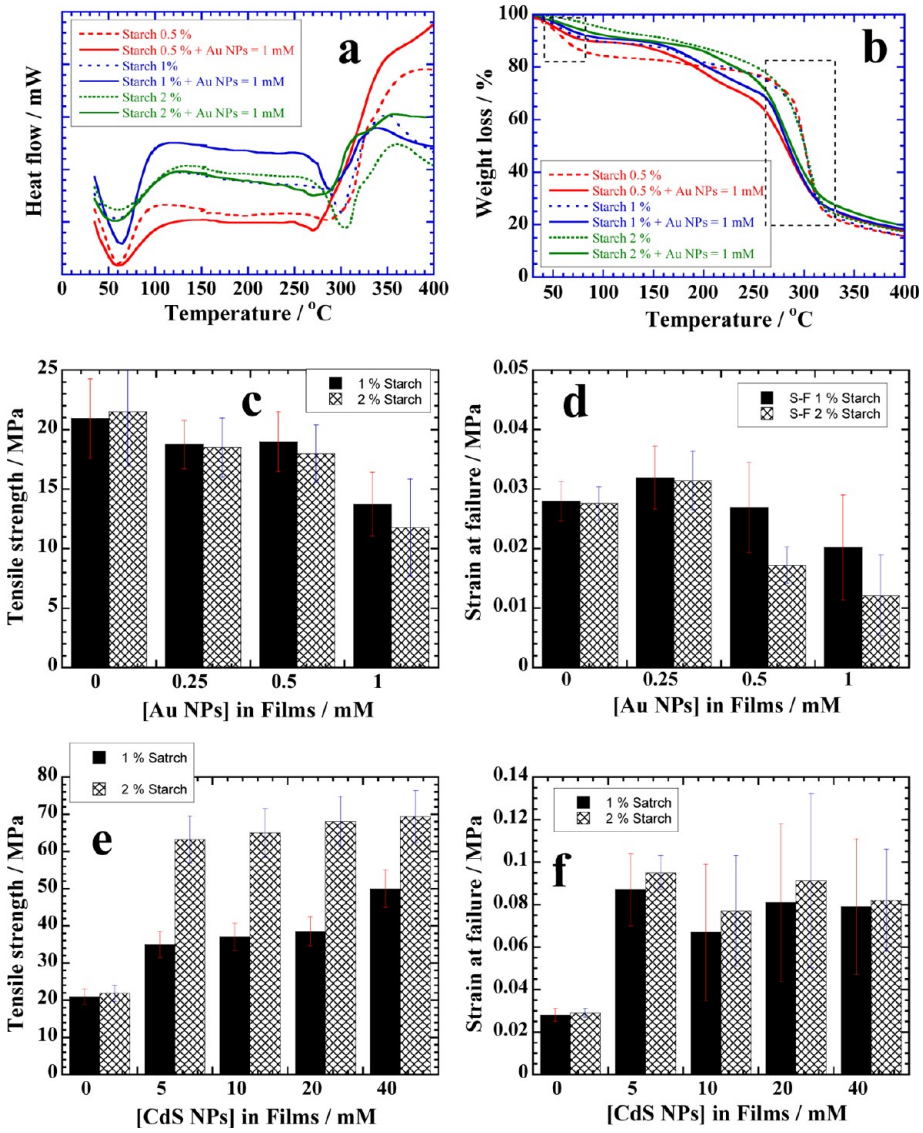

Figure 5. Heat flow (a) and weight loss (b) scans of starch films made with 0.5, 1, and 2% starch without and with Au NPs. Tensile strength (c) and strain at failure (d) plots of 1 and 2% starch films embedded with Au NPs versus the amount of NPs. Tensile strength (e) and strain at failure (f) plots of 1 and 2% starch films embedded with CdS NPs versus the amount of NPs. See details in the text.

NPs whereas that of the control (panel b) is relatively much more smooth with no sign of peaks. Panels c and d show the respective height images of the films where one can see the presence of groups of embedded NPs in panel c whereas again panel d gives an almost flat surface. Panel e provides the three-dimensional image with approximate height due to the embedded NPs which is slightly more than 100 nm and obviously expected in view of the thick coating of several layers of starch on NPs. Similar behavior is demonstrated by the film made with 2% starch (Supporting Information Figure S6).

DSC Studies. In view of the applications of present starch films in food and pharmaceutical industries as packaging materials, their thermal properties are required. Each film gives two endothermic peaks both in the absence as well as in the presence of NPs (Figure 5a). The first broad peak around 60 °C (Table 1) is considered to be due to the loss of entrapped water molecules in liquid crystalline phase of predominantly amylopectine region.[47] The broad nature of the peak is related to slow release of the entrapped moisture with a steady increase in temperature and accompanied by a relatively little amount of weight loss (see corresponding dotted box in Figure 5b) that increases with the amount of starch (i.e., 3, 8, and 15% weight loss for 0.5, 1, and 2% starch, respectively, for the films without NPs). Likewise endothermic enthalpy (ΔH) decreases with the increase in the hydration in the order of 0.5% > 1% > 2% starch

Table 1. Transition Temperatures and Endothermic Enthalpies of Starch Films without and with Au and CdS NPs

	peak$_1$ T(°C)	ΔH_1 (J/g)	peak$_2$ T(°C)	ΔH_2 (J/g)
0.5% starch	60.7	258.9	285	177.9
1% starch	59.9	193.7	303	106.8
2% starch	60.8	190.2	303	91.2
0.5% starch + 1 mM Au NPs	60.1	336.5	273	230.6
1% starch + 1 mM Au NPs	62.7	280.3	289	188.5
2% starch + 1 mM Au NPs	59.8	229.3	287	176.4
0.5% starch + 1 mM CdS NPs	60.7	352.8	279	58.6
1% starch + 1 mM CdS NPs	61.2	297.3	283	56.4
2% starch + 1 mM CdS NPs	70.6	179.4	267	24.2

dx.doi.org/10.1021/sc3000652 | ACS Sustainable Chem. Eng. 2013, 1, 127−136

(Table 1). In the presence of NPs, all peaks are more prominent and again appearing close to 60 °C but with higher ΔH values (Table 1) and comparatively less weight loss with respect to that in the absence of NPs. Stabilization of colloidal NPs in aqueous starch solution can be viewed in terms of DLVO theory[48,49] where electrostatic interactions between the starch hydroxyl groups and the charged nanometallic surface play a predominant role over the cohesive interactions due to van der Waals forces between the NPs. The former will replace previously associated water molecules in the starch superhelix to provide necessary colloidal stability that in turn reduces the effective amount of entrapped moisture in comparison to that in the absence of NPs. Hence, the films thus produced in the presence of NPs contain a lesser amount of moisture with a relatively greater amount of crystallinity.

The second peak appearing at >260 °C (Figure 5a) is due to the melting of starch chains followed by the decomposition of glucose rings under the effect of thermal decomposition[50,51] which is expected to release water most probably due to condensation among the neighboring −OH groups of predominantly hydrophilic amylopectin and even the formation of C═C. That is why the corresponding overall transition temperature is much higher than the first peak, and even higher for 1 or 2% in comparison to 0.5% starch (Table 1). Likewise ΔH values are much lower than the corresponding first peak with the same trend. In the presence of NPs, we obtained slightly lower transition temperature in comparison to their absence with higher ΔH values. Although the ultimate weight loss (i.e., ∼80%) is more or less the same in the absence as well as in the presence of NPs, the major difference is in their slopes (corresponding dotted area in Figure 5b). For pure starch films, the slopes are relatively steeper than in the presence of NPs, suggesting a rapid decomposition of glucose rings in the absence of NPs. Complexation with glucose rings makes this process relatively slower. Similar behavior is observed for CdS NPs embedded starch films (Supporting Information Figure S7).

Mechanical Properties. Mechanical properties help us to understand the workability and applicability of starch film and are best understood in terms of tensile strength and strain at failure (flexibility). Figure 5c and d demonstrate both properties for 1 and 2% starch in the presence of Au NPs. Tensile strength decreases with increasing amounts of Au NPs while flexibility improves with 0.25 mM NPs but decreases thereafter. Decrease in the tensile strength can be correlated with a higher degree of crystallinity in the presence of NPs as evident from the thermal properties (Figure 5a and b). However, increase in the flexibility with a small amount of NPs, i.e. 0.25 mM, can be attributed to a decrease in the hydrogen bonding[52] which is responsible for the superhelix arrangement among starch macromolecules. Greater hydrogen bonding generates stronger interhelical interactions with less flexibility and vice versa. A small amount of NPs can be accommodated in the mesh of interconnected starch macromolecules (strands) without significantly disturbing their helical arrangement, but a greater amount of NPs on the other hand disturbs the superhelix arrangement and thereby decreases the flexibility.

The presence of CdS NPs dramatically improves the mechanical properties. A significant increase in the tensile strength (Figure 5e) and flexibility (Figure 5f) is observed in the CdS NP incorporated starch films. Both tensile strength as well as flexibility increase with the increase in the amount of CdS NPs before tending to a constant value and are higher for 2% starch than 1%. This remarkable difference from that of Au NP incorporated films might have arisen from a different mode of synthesis of CdS NPs. Synthesis of CdS NPs has been carried out in the presence of glycerol medium, thus glycerol stabilized starch coated CdS NPs help to provide greater stability and flexibility.[53]

DISCUSSION

Present results demonstrate a systematic way of synthesizing NP incorporated biodegradable starch films. We want to show that the presence of NPs makes a significant difference in the strength and flexibility of starch films for their industrial applications in comparison to the films simply made with only starch (without NPs). We are mainly looking for their versatile applications in the packaging and pharmaceutical industries where biodegradable starch films should provide required strength, moisture barrier, and fluorescence activity for easy detection. Our results show that a systematic synthetic method as monitored by the UV−visible studies (Figure 1a−c) can be easily applied to produce starch stabilized Au NPs, which can simultaneously be incorporated into starch films. Such starch films are UV−visible active due to the presence of Au NPs (Figure 1d and f). Similar films can also be produced by incorporating fluorescence active CdS NPs. Incorporation of NPs in the superhelix arrangement of starch (Figure 6) induces

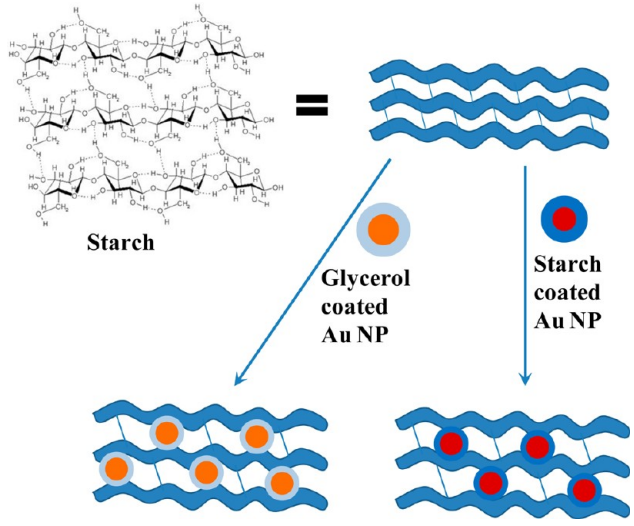

Figure 6. Schematic representation showing glucose units joined together by glycosidic bonds to construct a superhelix layered structured interlocked by hydrogen bonding. The lower part of the diagram shows intercalated starch capped Au NPs and glycerol capped CdS NPs among different layers. See details in the text.

significant influence on the mechanical properties of the starch films. Although Au NPs (Figure 5c and d) decrease the mechanical strength, their low amount increases the flexibility, while CdS NPs (Figure 5e,f) significantly increase the tensile strength as well as flexibility. Keeping in view of their almost similar dimensions, it all seems to be due to the different methods used in their synthesis. We believe that the stabilization of glycerol coated CdS NPs proves to be a better option rather than only starch coated Au NPs. Although glycerol has also been used as plasticizer in Au NP incorporated starch films, the lower tensile strength of such films in comparison to that of CdS NPs suggested poor intercalation of

glycerol molecules in the double helical arrangement of starch macromolecules. Therefore, NPs alone cannot increase the tensile strength as well as flexibility; it is the glycerol stabilized NPs which provide additional strength and flexibility.

In order to understand it further, we need first to understand the role of glycerol as a plasticizer.[54] Glycerol is a polyol with three hydroxyl groups. Addition of glycerol in starch reduces the direct hydrogen bonding between the different chains of starch macromolecules by incorporating among them. This increases the interhelical distance among different chains and increases the flexibility. When such places are occupied by the glycerol stabilized NPs whose dimensions are no doubt much greater than glycerol molecules, distances between the helical chains are further increased which in turn contributes toward even greater flexibility (Figure 6). Since the Au NPs are synthesized in the absence of glycerol medium (in the presence of aqueous starch), therefore they are expected to be already coated with predominantly crystalline starch (Figure 6) because the reactions are conducted at 70 °C where substantial dehydration is expected. This leaves little possibility for glycerol molecules to intercalate effectively in the already predominantly crystalline starch coating unlike that of CdS NPs which are synthesized only in the glycerol medium. Thus, NPs previously stabilized by glycerol prove to be better candidates for inducing greater flexibility among starch superhelix chains in comparison to NPs already stabilized by predominantly crystalline starch. This seems to be the key step in increasing both tensile strength as well as flexibility of starch films. Furthermore, the nature of the NP surface whether it is metallic or semiconductor probably does not matter because NPs properly coated and stabilized by glycerol produce films with better tensile strength and flexibility. The size of both kinds of NPs, i.e. Au and CdS, was within 25−100 nm for their effective accommodation and manipulation in the starch superhelix arrangement in order to generate greater stability in comparison to the films made in their absence. A much larger size of ca. 0.5 μm or more than this is considered to significantly disturb the helical arrangement thereby adversely affecting the flexibility or tensile strength of the films. Thus, a smaller size of NPs as used in the present study works well in achieving better film properties best suited for various industrial applications.

■ ASSOCIATED CONTENT

Supporting Information

UV−visible spectra, TEM, AFM, and DSC scans. This material is available free of charge via the Internet at http://pubs.acs.org.

■ AUTHOR INFORMATION

Corresponding Author

*E-mail address: ms_bakshi@yahoo.com.

Notes

The authors declare no competing financial interest.

■ ACKNOWLEDGMENTS

These studies were partially supported by financial assistance under Article 23.7.1 of the CAS agreement of WLU, Waterloo. G.K. thankfully acknowledges the financial support provided by the Research and Development Council (RDC) of Newfoundland and Labrador, NSERC, and the Office of Applied Research at CNA.

■ REFERENCES

(1) Mullen, J. W.; Pacsu, E. Starch studies: possible industrial utilization of starch esters. *Ind. Eng. Chem.* **1942**, *34*, 1209−1217.
(2) Thurber, F. H. Chemical and Physical Properties of Sweet Potato Starch. *Ind. Eng. Chem.* **1933**, *25*, 565−568.
(3) Singh, V.; Okadome, H.; Toyoshima, H.; Isobe, S.; Ohtsubo, K. Thermal and physicochemical properties of rice grain, flour and starch. *J. Agric. Food Chem.* **2000**, *48*, 2639−2647.
(4) Torres, F. G.; Troncoso, O. P.; Torres, C.; Diaz, D. A.; Amaya, E. Biodegradability and mechanical properties of starch films from Andean crops. *Int. J. Biol. Macromol.* **2011**, *48*, 603−606.
(5) Sun, S.; Mitchell, J. R.; Macnaughtan, W.; Foster, T. J.; Harabagiu, V.; Song, Y.; Zheng, Q. Comparison of the Mechanical Properties of Cellulose and Starch Films. *Biomacromolecules* **2009**, *11*, 126−132.
(6) Singh, N.; Belton, P. S.; Georget, D. M. The effects of iodine on kidney bean starch: Films and pasting properties. *Int. J. Biol. Macromol.* **2009**, *45*, 116−119.
(7) Bastos, D. C.; Santos, A. E.; da Silva, M. L.; Simao, R. A. Hydrophobic corn starch thermoplastic films produced by plasma treatment. *Ultramicroscopy* **2009**, *109*, 1089−1093.
(8) Lafargue, D.; Pontoire, B.; Buleon, A.; Doublier, J. L.; Lourdin, D. Structure and mechanical properties of hydroxypropylated starch films. *Biomacromolecules* **2007**, *8*, 3950−3958.
(9) Shogren, R. Effect of orientation on the physical properties of potato amylose and high-amylose corn starch films. *Biomacromolecules* **2007**, *8*, 3641−3645.
(10) Viguie, J.; Molina-Boisseau, S.; Dufresne, A. Processing and Characterization of Waxy Maize Starch Films Plasticized by Sorbitol and Reinforced with Starch Nanocrystals. *Macromol. Biosci.* **2007**, *7*, 1206−1216.
(11) Mathew, S.; Brahmakumar, M.; Abraham, T. E. Microstructural imaging and characterization of the mechanical, chemical, thermal, and swelling properties of starch−chitosan blend films. *Biopolymers* **2006**, *82*, 176−187.
(12) Ononokpono, O. E.; Spring, M. S. The effects of inclusions and conditions of storage on the mechanical properties of maize starch and methylcellulose films. *J. Pharm. Pharmacol.* **1988**, *40*, 313−319.
(13) Tongdeesoontorn, W.; Mauer, L. J.; Wongruong, S.; Sriburi, P.; Rachtanapun, P. Effect of carboxymethyl cellulose concentration on physical properties of biodegradable cassava starch-based films. *Chem. Cent. J.* **2011**, *5*, 6.
(14) Pyla, R.; Kim, T. J.; Silva, J. L.; Jung, Y. S. Enhanced antimicrobial activity of starch-based film impregnated with thermally processed tannic acid, a strong antioxidant. *Int. J. Food Microbiol.* **2010**, *137*, 154−160.
(15) Wu, C. S. Characterizing biodegradation of PLA and PLA-g-AA/starch films using a phosphate-solubilizing bacillus species. *Macromol. Biosci.* **2008**, *8*, 560−567.
(16) Henrique, C. M.; Teofilo, R. F.; Sabino, L.; Ferreira, M. M.; Cereda, M. P. Classification of Cassava Starch Films by Physicochemical Properties and Water Vapor Permeability Quantification by FTIR and PLS. *J. Food Sci.* **2007**, *72*, E184−E189.
(17) Yakimets, I.; Paes, S. S.; Wellner, N.; Smith, A. C.; Wilson, R. H.; Mitchell, J. R. Effect of water content on the structural reorganization and elastic properties of biopolymer films: a comparative study. *Biomacromolecules* **2007**, *8*, 1710−1722.
(18) Cervera, M. F.; Karjalainen, M.; Airaksinen, S.; Rantanen, J.; Krogars, K.; Heinamaki, J.; Colarte, A. I.; Yliruusi, J. Physical stability and moisture sorption of aqueous chitosan-amylose starch films plasticized with polyols. *Eur. J. Pharm. Biopharm.* **2004**, *58*, 69−76.
(19) Krogars, K.; Heinamaki, J.; Karjalainen, M.; Niskanen, A.; Leskela, M.; Yliruusi, J. Enhanced stability of rubbery amylose-rich maize starch films plasticized with a combination of sorbitol and glycerol. *Int. J. Pharm.* **2003**, *251*, 205−208.
(20) Ononokpono, O. E.; Spring, M. S. The effects of inclusions and conditions of storage on the mechanical properties of maize starch and methylcellulose films. *J. Pharm. Pharmacol.* **1988**, *40*, 313−319.

(21) Yao, Y.; Zhang, J.; Ding, X. Partial beta-amylolysis retards starch retrogradation in rice product. *J. Agric. Food Chem.* **2003**, *51*, 4066−4071.
(22) Kohyama, K.; Nishinari, K. Effect of soluble sugars on gelatinization and retrogradation of sweet potato starch. *J. Agric. Food Chem.* **1991**, *39*, 1406−1410.
(23) Yao, Y.; Zhang, J.; Ding, X. Structure-retrogradation relationship of rice starches in purified starches and cooked rice grains: a statistical investigation. *J. Agric. Food Chem.* **2002**, *50*, 7420−7425.
(24) Bakshi, M. S. Nanoshape Control Tendency of Phospholipids and Proteins: Protein−Nanoparticle Composites, Seeding, Self-Aggregation, and Their Applications in Bionanotechnology and Nanotoxicology. *J. Phys. Chem. C* **2011**, *115*, 13947−13960.
(25) Bakshi, M. S.; Kaur, H.; Khullar, P.; Banipal, T. S.; Kaur, G.; Singh, N. Protein Films of Bovine Serum Albumen Conjugated Gold Nanoparticles: A Synthetic Route from Bioconjugated Nanoparticles to Biodegradable Protein Films. *J. Phys. Chem. C* **2011**, *115*, 2982−2992.
(26) Bakshi, M. S.; Kaur, H.; Banipal, T. S.; Singh, N.; Kaur, G. Biomineralization of Gold Nanoparticles by Lysozyme and Cytochrome c and Their Applications in Protein Film Formation. *Langmuir* **2010**, *26*, 13535−13544.
(27) Le Corre, D. ü.; Bras, J.; Dufresne, A. Starch Nanoparticles: A Review. *Biomacromolecules* **2010**, *11*, 1139−1153.
(28) He, F.; Zhao, D. Preparation and Characterization of a New Class of Starch-Stabilized Bimetallic Nanoparticles for Degradation of Chlorinated Hydrocarbons in Water. *Environ. Sci. Technol.* **2005**, *39*, 3314−3320.
(29) Sereno, N. M.; Hill, S. E.; Taylor, A. J.; Mitchell, J. R.; Davies, S. J. Aroma Permeability of Hydroxypropyl Maize Starch Films. *J. Agric. Food Chem.* **2009**, *57*, 985−990.
(30) Hoagland, P. D. Films from Pectin, Chitosan, and Starch. *Macromolecular Interactions in Food Technology*, 650 ed.; American Chemical Society: Washington, D.C., 1996; pp 145−154.
(31) Coffin, D. R.; Fishman, M. L. Mechanical Properties of Pectin—Starch Films. *Polymers from Agricultural Coproducts*, 575 ed.; American Chemical Society: Washington, D.C., 1994; pp 82−91.
(32) Sommerfeld, H.; Blume, R. Biodegradable films. Based on partially hydrolyzed corn starch or potato starch. *J. Chem. Educ.* **1992**, *69*, A151.
(33) Bakshi, M. S.; Sachar, S.; Kaur, G.; Bhandari, P.; Kaur, G.; Biesinger, M. C.; Possmayer, F.; Petersen, N. O. Dependence of Crystal Growth of Gold Nanoparticles on the Capping Behaviour of Surfactant at Ambient Conditions. *Cryst. Growth Des.* **2008**, *8*, 1713−1719.
(34) Bakshi, M. S. A Simple Method of Superlattice Formation: Step − by − Step Evaluation of Crystal Growth of Gold Nanoparticles through Seed − Growth Method. *Langmuir* **2009**, *25*, 12697−12705.
(35) Williams, P. C.; Kuzina, F. D.; Hlynka, I. A rapid colorimetric procedure for estimating the amylase content of starches and flours. *Cereal Chem.* **1970**, *47*, 411.
(36) Khullar, P.; Singh, V.; Mahal, A.; Kaur, H.; Singh, V.; Banipal, T. S.; Kaur, G.; Bakshi, M. S. Tuning Shape and Size of Gold Nanoparticles with Triblock Polymer Micelle Structure Transitions and Environments. *J. Phys. Chem. C* **2011**, *115*, 10442−10454.
(37) Khullar, P.; Mahal, A.; Singh, V.; Banipal, T. S.; Kaur, G.; Bakshi, M. S. How PEO-PPO-PEO Triblock Polymer Micelles Control the Synthesis of Gold Nanoparticles: Temperature and Hydrophobic Effects. *Langmuir* **2010**, *26*, 11363−11371.
(38) Yao, W. T.; Yu, S. H.; Liu, S. J.; Chen, J. P.; Liu, X. M.; Li, F. Q. Architectural control syntheses of CdS and CdSe nanoflowers, branched nanowires, and nanotrees via a solvothermal approach in a mixed solution and their photocatalytic property. *J. Phys. Chem. B* **2006**, *110*, 11704−11710.
(39) Lakowicz, J. R.; Gryczynski, I.; Piszczek, G.; Murphy, C. J. Emission Spectral Properties of Cadmium Sulfide Nanoparticles with Multiphoton Excitation. *J. Phys. Chem. B* **2002**, *106*, 5365−5370.
(40) Bakshi, M. S.; Kaur, G.; Thakur, P.; Banipal, T. S.; Possmayer, F.; Petersen, N. O. Surfactant Selective Synthesis of Gold Nanowires by Using DPPC-Surfactant Mixture as Capping Agent at Ambient Conditions. *J. Phys. Chem. C* **2007**, *111*, 5932−5940.
(41) Bakshi, M. S.; Possmayer, F.; Petersen, N. O. Role of Different Phospholipids in the Synthesis of Pearl-Necklace Type Gold-Silver Bimetallic Nanoparticles as Bioconjugate Materials. *J. Phys. Chem. C* **2007**, *111*, 14113−14124.
(42) Bakshi, M. S. NanoShape Control Tendency of Phospholipids and Proteins: Protein − Nanoparticles composites, Seeding, Self-aggregation, and their Applications in Bio-nanotechnology and Nanotoxicology. *J. Phys. Chem. C* **2011**, *115*, 13947−13960.
(43) Das, K.; Ray, D.; Bandyopadhyay, N. R.; Gupta, A.; Sengupta, S.; Sahoo, S.; Mohanty, A.; Misra, M. Preparation and Characterization of Cross-Linked Starch/Poly(vinyl alcohol) Green Films with Low Moisture Absorption. *Ind. Eng. Chem. Res.* **2010**, *49*, 2176−2185.
(44) Talja, R. A.; Peura, M.; Serimaa, R.; Jouppila, K. Effect of amylose content on physical and mechanical properties of potato-starch-based edible films. *Biomacromolecules* **2008**, *9*, 658−663.
(45) Lafargue, D.; Pontoire, B.; Buleon, A.; Doublier, J. L.; Lourdin, D. Structure and mechanical properties of hydroxypropylated starch films. *Biomacromolecules* **2007**, *8*, 3950−3958.
(46) Qin, F.; Man, J.; Xu, B.; Hu, M.; Gu, M.; Liu, Q.; Wei, C. Barley Grain Constituents, Starch Composition, and Structure Affect Starch in Vitro Enzymatic Hydrolysis. *J. Agric. Food Chem.* **2011**, *59*, 12667−12673.
(47) Chel-Guerrero, L.; Betancur, A. D. Cross-linkage of Canavalia ensiformis starch with adipic acid: chemical and functional properties. *J. Agric. Food Chem.* **1998**, *46*, 2087−2091.
(48) Levine, S.; Dube, G. P. Interaction between two hydrophobic colloidal particles, using the approximate Debye-Huckel theory. I. General properties. *Trans. Faraday Soc. 35* **1940**, *114*, 1125.
(49) Derjaguin, B.; Landau, L. Theory of the stability of strongly charged lyophobic sols and of the adhesion of strongly charged particles in solutions of electrolytes. *Acta Physico Chemica URSS* **1941**, *14*, 633.
(50) Nie, S.; Song, L.; Guo, Y.; Wu, K.; Xing, W.; Lu, H.; Hu, Y. Intumescent Flame Retardation of Starch Containing Polypropylene Semibiocomposites: Flame Retardancy and Thermal Degradation. *Ind. Eng. Chem. Res.* **2009**, *48*, 10751−10758.
(51) Das, K.; Ray, D.; Bandyopadhyay, N. R.; Gupta, A.; Sengupta, S.; Sahoo, S.; Mohanty, A.; Misra, M. *Ind. Eng. Chem. Res.* **2010**, *49*, 2176−2185.
(52) Sun, S.; Mitchell, J. R.; MacNaughtan, W.; Foster, T. J.; Harabagiu, V.; Song, Y.; Zheng, Q. Comparison of the Mechanical Properties of Cellulose and Starch Films. *Biomacromolecules* **2009**, *11*, 126−132.
(53) Angles, M. N.; Dufresne, A. Plasticized starch/tunicin whiskers nanocomposites: 2. Mechanical behavior. *Macromolecules* **2001**, *34*, 2921−2931.
(54) Gao, C.; Stading, M.; Wellner, N.; Parker, M. L.; Noel, T. R.; Mills, E. N. C.; Belton, P. S. Plasticization of a protein-based film by glycerol: a spectroscopic, mechanical, and thermal study. *J. Agric. Food Chem.* **2006**, *54*, 4611−4616.